A Computer-Aided Approach for Designing Edge-Slot Waveguide Arrays

R.B. Gosselin
Microwave Instrument Technology Branch, Code 555
NASA - Goddard Space Flight Center
Greenbelt, MD 20771, U.S.A.

Abstract: **Traditional techniques for designing resonant edge-slot waveguide arrays have required an iterative trial-and-error process of measuring slot data from several prototypes. Since very little meaningful data has been published, this technology remains relatively immature and prohibitive for many smaller programs that could benefit from some advantages this antenna has to offer. A new Computer-Aided Design technique for designing resonant edge-slot waveguide arrays was used to successfully design such an X-band radiometer antenna for the NASA Light Rainfall Radiometer (LRR) instrument. Having the ability to rapidly create such an extremely accurate and efficient antenna design without the need to manufacture prototypes has also enabled inexpensive research that promises to improve the system-level performance of microwave radiometers for upcoming space-flight missions. This paper will present details of the LRR antenna design and describe some other current edge-slot array accomplishments at Goddard Space Flight Center.**

1. Introduction

The recent success of NASA's Light Rainfall Radiometer (LRR) aircraft mission has demonstrated some tremendous advantages of resonant edge-slot waveguide arrays for passive microwave Synthetic Aperture Interferometric Radiometry (SAIR) applications **[1, 2]**. The quality of science data received during several test flights can be attributed in part to the very high-performance of the fourteen X-band antenna elements mounted beneath the aircraft. Because of their incredible mechanical integrity it was possible to fly them using only a very thin layer of Kapton tape over the openings and a dry-nitrogen purge to remove potential accumulations of moisture. Achieving such high-quality antenna performance using a computer-aided approach and eliminating the effects of a radome was an important accomplishment for passive microwave radiometry and has it renewed interest in exploring edge-slot waveguide array technology for future space-flight missions.

Despite what these antennas have to offer, they have never emerged as an off-the-shelf technology primarily because it remains very difficult to determine the precise slot depths and angles to produce an optimized design. The choice of this antenna on a previous L-band program proved to be a very expensive one especially when burdened with some of the common design issues and the absence of literature offering reliable engineering guidelines **[3,4].** In many cases the huge benefits of having an extremely low-loss, integrated waveguide combiner network have been lost to the accumulated design inaccuracies.

LRR was an example of a small project with very limited funding that leveraged from a commercially available electromagnetic software package to overcome these past obstacles. In this case the commercial software used was Ansoft HFSS (http://www.ansoft.com). It replaced the expensive and time-consuming empirical techniques from the past with virtual models that simply required a moderate amount of computer resources. No longer was it necessary to manufacture and measure numerous prototype antennas to characterize slot performance The time to derive the set of design curves for resonant slot characteristics at X-band was less than the time spent on a previous program to achieve just one data-point at a more forgiving L-Band frequency.

2. Basic Design Principles [7, 8, 9, 10]:

A section from a typical resonant edge-slot waveguide array is shown in **Figure 1**. The basic approach for designing them has remained unchanged since the first radar applications of WWII **[3,5]**. Slots are machined across the narrow face of the waveguide at some alternating fixed angles $\pm\theta$ to interrupt the currents along the inside skin so radiation propagates from an electric field vector bridging that gap. The resulting slot also penetrates into each of the broad-walls by some depth d; which LRR defined in accordance with the typical convention as measured with respect to the outside surface of the narrow wall being cut.

Figure 2 shows a graphical visualization using Ansoft HFSS to display radiation from a slot in terms of electric field vectors. Slots are located at half-guide-wavelength intervals where standing-wave energy inside the waveguide is peaked between the shorting plates at each end. **Figure 3** shows a cross-sectional contour plot of radiation inside the waveguide and slots using HFSS post-processing of the antenna; and this graphical representation was an especially useful diagnostic tool to provide confidence that microwave propagation inside the waveguide was correctly aligned with the slot locations.

Adjusting slot angle is the common technique for controlling the amount of radiation from a slot. For example, a tapered array design requires placement of the largest slot angles at the array center since these excitations are the greatest, and the angles must be progressively decreased towards each end. Different slot depths are necessary for each slot angle in order to maintain resonance. The analogy between slots and the complimentary dipole provides a good explanation why maintaining some constant resonant slot length requires that the contribution from the wrap-around depth penetrating into the broad-wall must decrease as slot angle increases and vice-versa **[6].**

Some interesting work has been done by others to achieve variable radiation from a slot by adjusting obstacles and irises inside the waveguide; however the possibility of further reducing bandwidth and adding to the mechanical complexity of the LRR array made this option less attractive for LRR. This past work emphasizes the fact that these types of antennas incorporate the internal RF combiner network as part of the external radiating structure and there is essentially no isolation allowing a partition between the two designs.

3. Design Approach Used for LRR Antennas:

Using data from resonant slots and applying the basic concept of pure conductances in parallel (as described by the ladder-line model shown in **Figure 4)** was the fundamental approach for the LRR design effort. To derive individual slot conductance directly from the array S11, the average individual slot conductance was calculated as the conductance measured for the entire array divided by the number of slots.

A series of models having progressive increments of deeper slots were created and analyzed until the admittance (derived from the S11) for the array had only a very small contribution from the susceptance term and crossed over the line of pure conductance when plotted on a Smith Chart. This technique was used to derive a summary of slot data from several uniform 36-slot array models using HFSS, and the results for first resonances at various angles are documented in the design curves of **Figure 5** and **Figure 6.**

Using the HFSS modeling approach had the advantage that S11 was provided from a single waveguide port definition as shown in **Figures 7 and 8** and therefore the slot characteristics were not masked by the sometimes complicated electrical effects of a probe assembly. This departs from the traditional feed-point shown for the ladder line in **Figure 5**; which is based on the actual hardware representation with a feed shown in **Figure 9.** Past laboratory techniques

typically only measured incremental slot conductance of an array by covering a single slot with copper tape and subtracting this value from what was measured previously with the slot uncovered **[10]**.

Once a database of slot characteristics (as represented by the curves shown in **Figures 5** and **6** was established, any array design could easily be created using a spreadsheet with the desired voltage distribution coefficients as input. Embedded in this approach is the assumption that mutual coupling changes between neighboring slots of slightly differing angles will have negligible impact. To minimize the potential impact of errors caused by mutual coupling, the uniform array models created to derive the design curves used the same number of slots (36) as the final tapered design.

Creating a well-matched array of uniform linear voltage excitations is usually somewhat simple since there is only one common value of angle theta and depth d for each and every slot. To achieve a reasonable match to the waveguide characteristic impedance, each resonant slot in a uniform array must have a normalized conductance value close to 1/N where N equals the number of slots in the array. This follows from the general rule that to achieve a good array match the sum of the normalized conductances must sum to 1.0 **[7]**. Making a Uniform array is especially easy if there is no firm length requirement so the number of slots can be adjusted.

The array excitations for the final LRR antenna slots were defined using the Villeneuve array equations to create a-Taylor 25 dB, nBar=4 **[11]**. The desired slot conductances $\mathbf{g_n}$ for each array element were applied to a spreadsheet **(Table 1)** that used data from **Fig. 5 and Fig. 6** to compute each of the 36 resonant slot angles and depths. Some design limitations did occur for two end-elements where the curves are not defined for smaller values of slot angle since resonance was no longer achievable. The slot angle and depth for the third and thirty-forth slots were simply copied for those adjacent end locations since only small errors were anticipated because they were not contributing much radiation. This deviation also seemed acceptable since these edge-elements may have been prone to small errors from mutual coupling effects anyway. It is interesting to consider, however, the mutual coupling effects between slots of shallower angles (lower conductance) should be less pronounced and may be the reason why the curve for slot depth in **Figure 6** has a sharply increase. Likewise, at these small angles there is closer agreement between the curves in **Figure 10** labeled "HFSS Resonant Uniform Array of 36 slots" and "Watson's Ordinary Conductance" which was intended for characterization of end-slots **[7]**.

Table 1 uses **Equation 1** to define the normalized conductances for each slot from the desired aperture taper voltage coefficients **[7]**.

$$g_n = \frac{a_n^2}{\sum_{i=1}^{t} a_i^2} \qquad (1)$$

Where $\mathbf{g_n}$ is the individual normalized slot conductance, **t** is the total number of slots, **n** is the slot number, and $\mathbf{a_n}$ is the coefficient for slot excitation voltage defined by the taper. **Equation 1** is derived from the relationship that the square of the voltage excitation at each slot is proportional to the normalized conductance, and enforces the requirement that for a matched end-fed array as shown in **Figure 9** the sum of those slot conductances must equal one to properly match the slots to the characteristic impedance of the waveguide.

4. LRR Antenna Performance:

The first LRR antenna produced used a typical probe though the broad-wall with tuning screws on the opposite side. To adjust these screws to match the probe, the slots were sealed with copper foil tape and a terminating load was used in place of the shorting plate at the end furthest from the probe. The two tuning screws were adjusted and locked once VSWR displayed on the Network Analyzer indicated an excellent match. The tape was removed from the slots and the load was replaced by the shorting plate. The evidence of a well optimized array design was indicated by the excellent match at the center frequency; which remained unchanged. Typical VSWR performance for two adjacent waveguide arrays is shown in **Figure 11**. . The VSWR typically did shift slightly when the LRR arrays are placed in the instrument-array environment with identical neighboring elements in close proximity; however for all fourteen sticks it typically remained less than 1.16:1 over the band of 10.65 GHz to 10.85 GHz.

Typical cross-polarized and co-polarized azimuth patterns for the series of manufactured LRR arrays are shown in **Figure 12** and **Figure 13,** respectively. The resulting side-lobe level was very close to the goal of -25 dB. It was fortunate that the slot angles for most of the 36 slots were very small since this minimized the cross-polarized lobes at approximately 42 degrees and therefore none of the typical techniques for reducing cross-pol. radiation were necessary for LRR **[4,10,12].**

5. Historical Comparison:

Prior to validation from the hardware fabrication and successful performance it was understood that comparison and agreement with past data was very important. **Figures 5 and 6** include resonant slot data for the LRR frequency of 10.7 GHz using both WR-75 and WR-90 waveguide, and for 9.375 GHz using only WR-90 waveguide. The 9.375 GHz case was constructed since it offers an interesting comparison with the WR-90 at 10.7 GHz case, and is a benchmark from what has often been published. **Figure 10** offers a direct comparison with some commonly published data and includes an overlay of the same HFSS curve for 9.375 GHz taken from **Figure 5**. **[7]**

6. Array Layout:

To minimize the accumulation of small errors, some special consideration was given to using several significant digits when defining array length and the precise location of the slots. The center frequency of 10.7 GHz translated into a guide-wavelength of roughly 1.63 inches inside the WR-75 tubing and meant the half-wave spacing between slots should be approximately 0.739 times the free-space wavelength. This unavoidable, but typical, violation of the Nyquist criteria was not an issue because the main beam remains stationary. Since the HFSS models assumed a perfectly square corner, the value for guide-wavelength which the software computed was extremely close to the standard text-book equation. This consistently close agreement gave some confidence to using that standard value for all the HFSS models. In the transition from software model to hardware, the value for lambda-guide and resulting slot spacing was recalculated to take into account some small effects of the radius at the waveguide edges that were not practical to model using HFSS **[13, 14]**.

The beamwidth requirements of the LRR instrument dictated that mechanical layout of the LRR array be determined prior to starting any electrical analyses and achieving a linear aperture of approximately 1 meter was a priority. The decision was made to use WR-75 waveguide since the alternative WR-90 type had a wider narrow-wall which exceeded the tight allowance for some of the interferometer spacings between adjacent linear arrays. From these factors it was calculated that 36 slots were necessary to adequately populate the aperture with some distance left between the feed probe and the first slot. One of the potential effects from a probe assembly is the presence of modes other than TE_{10}. To minimize any potential problems from moding that will alter the nearby slot conductances, a spacing distance of 3 guide-wavelengths from the probe to the first slot was part of the final LRR design shown in **Figure 9 [10, 16].**

In computing the necessary slot conductances it was somewhat fortunate that only two end-slots were outside the range of achievable values found in the derived curves of **Figures 5 and 6**. Such a limitation to the lowest value of resonant slot conductance can also be a restriction to maximum number of slots and overall length of the array.

7. Limitations and Future Work:

Some current investigations are attempting to better understand what influences the achievable range of slot conductances so compensations can be made when necessary. For example, the optimal slot width and waveguide wall thickness has been totally ignored by the literature but some experience using HFSS indicates they both very critical to slot performance. The Microwave Instrument Technology Branch at Goddard Space Flight Center is currently leading the design effort for a much more complicated edge-slot array operating at 36.5 GHz. Controlling the values for slot conductance has been a primary challenge driven by the requirement that the K_a-band array length must be 1.12 Meters; which is electrically much longer than the LRR X-band model that was at approximately 1 Meter. It has already been concluded that the nominal 40 Mil wall thickness of WR-22 must be reduced to 10 Mils to achieve any slot resonance at this higher frequency.

Larger array lengths inherently have narrower bandwidths, and this can lead to some interesting trade-offs when one considers the prospects of subdividing the array into sub-arrays. An HFSS analysis of the entire array of 184 slots has confirmed that for a maximum VSWR of 1.2:1, the bandwidth was approximately 20 MHz and fell short of the goal of 100 MHz. Breaking the antenna into two sub-arrays should offer some improvements; however implementing an external combiner network will add some complexity to the design. The simplest approach of using coaxial components is not an option because of the losses incurred. Center-feeding the antenna introduces the difficulty of disturbing slot performance near the feed probe assembly and the detrimental effect of sidelobes caused by simply removing them from the center of the array. Some complex arrangements of a waveguide feed network behind the array to feed each sub-array at the very ends seems to be most promising approach to ensure there is no gap between slots at the overall array center.

Looking ahead to the possibility of further subdividing the array into 4 sub-arrays presents some even greater engineering challenges. **Figure 14** is a plot of the conductance values necessary for a 25 dB, nBar=4 Taylor distribution applied over 4 sub-arrays using a power divider of equal amplitude and phase. The

unequal division of slots must be made to satisfy all the basic criteria for matching each sub-array design and the constraints defined by the taper including minimizing the discontinuity in conductance values between the middle and end sub-arrays. In this example, an overall array of 184 slots as shown in **Figure 14** would require a sub-array of 66 slots on each end; which may still be a large enough number to present some bandwidth issues. An alternative to this approach would be an unequal split in power that would allow the number of slots to be partitioned more evenly.

8. Conclusion:

The successful delivery of a low-cost, but very well-optimized antenna has proven that commercial computer tools have evolved to accurately predict the performance of edge-slot waveguide arrays. The knowledge gained from the LRR program has enabled some very accurate research that promises to improve passive microwave radiometry performance for an upcoming space-flight mission and should benefit edge-slot waveguide array technology in general.
The future of edge-slot technology seems very promising. A simple cut to form a slot through a piece of waveguide was at the threshold of technology during WWII, but there is reason for speculation that an evolution to more complex shapes and sizes could offer some performance improvements. The continued advances in computing power, Genetic Algorithm approaches **[15]**, and commercially available software offer some interesting prospects.

9. Acknowledgment:

.This work has been funded by the NASA Office of Earth Science and was made possible by the kind inspiration and generous support of the Microwave Instrument Technology Branch at NASA Goddard Space Flight Center.

References

[1] C. Ruf, et al., "Lightweight Rainfall Radiometer STAR Aircraft Sensor", International Geoscience and Remote Sensing Symposium, 2002.IEEE, Volume: 2 , 2002.

[2] R. B. Gosselin, S. E. Seufert, L.R. Dod, "Design of a Resonant Edge-Slot Waveguide Array for the Lightweight Rainfall Radiometer (LRR)", International Geoscience and Remote Sensing Symposium, 2003.IEEE

[3] S. R. Rengarajan, ., L. G. Josefsson, , R. S. Elliott "Waveguide-fed Slot Antennas and Arrays: A Review", Electromagnetics, Vol. 19, No. 1, January/February, 1999.

[4] M. M. Brady, "Single Slotted-Waveguide Linear Arrays" in Advances in Microwaves, L. Young, ed. New York: Academic Press, 1971.

[5] W. H.Watson, "The Physical Principles of Waveguide Transmission and Antenna Systems", Oxford University Press, London and New York, 1947.

[6] H. G. Booker, "Slot Aerials", J. Inst. Elect. Eng., Part 3 **93**, 42 (1946).

[7] H. Y. Yee, R. C. Voges, "Slot-Antenna Arrays", Chapter 9 in Antenna Engineering Handbook, 3rd Edition, eds. R. C Johnson, H. Jasik, New York: McGraw Hill, Inc.

[8] R. S. Elliott, "The Design of Waveguide-Fed Slot Arrays', Chapter 12 in Antenna Handbook, eds. Y. T. Lo, S. W. Lee, New York, Van Nostrand Reinhold Company, Inc.

[9] R. C. Hansen, "Linear Arrays", Chapter 9 in The Handbook of Antenna Design, Volume 2, eds. A. W. Rudge, K. Milne, A. D. Olver, P. Knight, London, UK., Peter Peregrinus Ltd.

[10] M .J. Ehrlich, "Slot-Antenna Arrays", Chapter 9 in Antenna Engineering Handbook, 1st Edition, ed. H. Jasik, New York: McGraw Hill Book Co., Inc.

[11] A. T. Villeneuve, "Taylor Patterns for Discrete Arrays", Antennas and Propagation, IEEE Transactions, Volume: 32 No. 10 , Oct 1984, Page(s): 1089 -1093.

[12] S. Matsuda, T. Takeshima, and Y. Isogai, "Crosspolarized Radiation Beams of Slot Array Antennas", Elec. Commun. Jap. 47, 77-84 (1964).

[13] D. M. Kerns and W. T. Grandy, "Pertubation Theorums for Waveguide Junctions, with Applications", IEEE Trans., Vol. MTT-14, No. 2. pp. 85-92 (February 1966).

[14] M. M. Brady, "Tables of Constants for Standard Rectangular Waveguides" in Microwave engineers' handbook. Volume 1. Compiled and edited by T. S. Saad. Co-editors: R. C. Hansen [and] G. J. Wheeler, T. S Saad, ed., pp. 38-71, Dedham, Mass., Artech House [1971].

[15] P. James, and S. J. Vetterlein, "A Wideband Resonant Slotted Waveguide Array for Space SAR Applications", NCAP 1998

[16] M.C. Bailey, Private Communication, NASA Langley Research Center, 1996.

Figure 1 - LRR Edge-Slot Waveguide Array

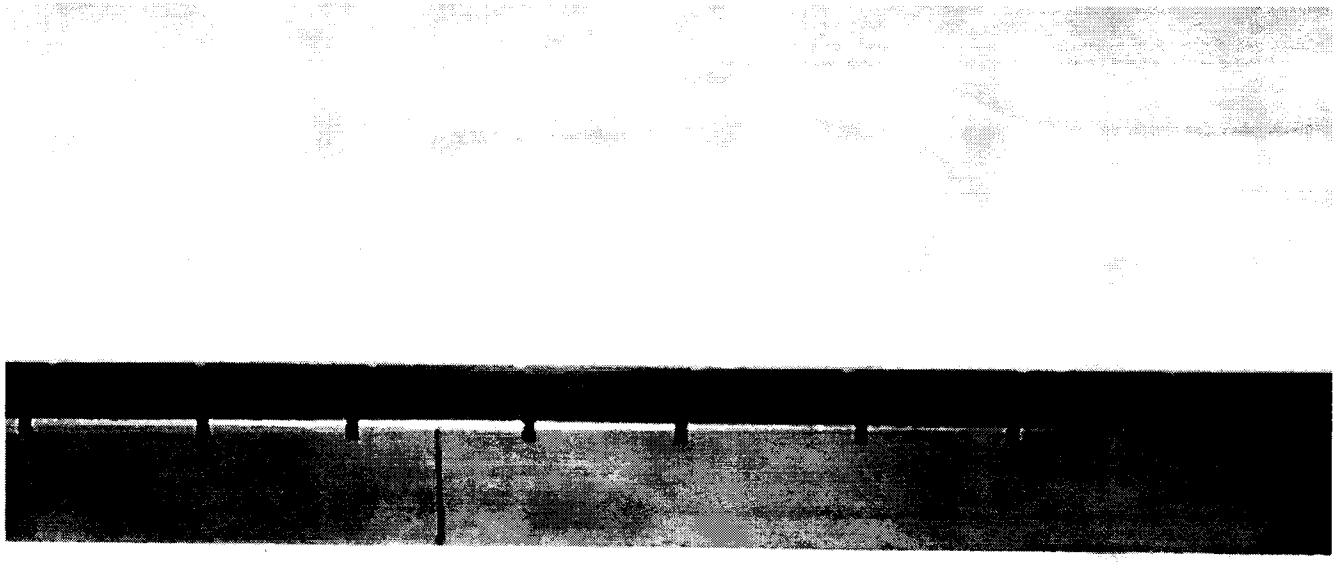

Figure 2 - HFSS Graphic of Slot Radiation

Figure 3 – HFSS-generated Contour Plot showing internal E-field Alignment with Slots

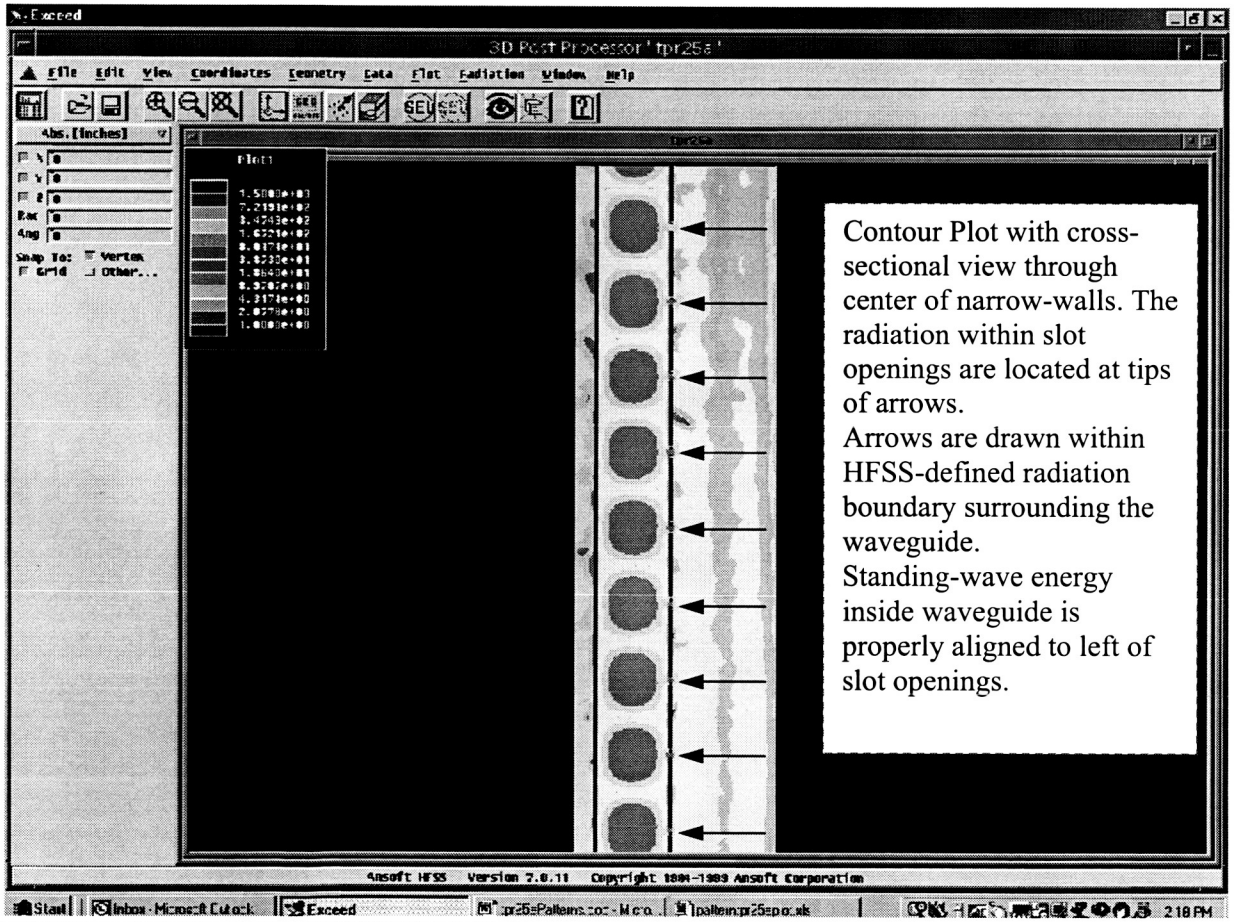

Figure 4 - Wire-line model of Slot Conductance in Parallel

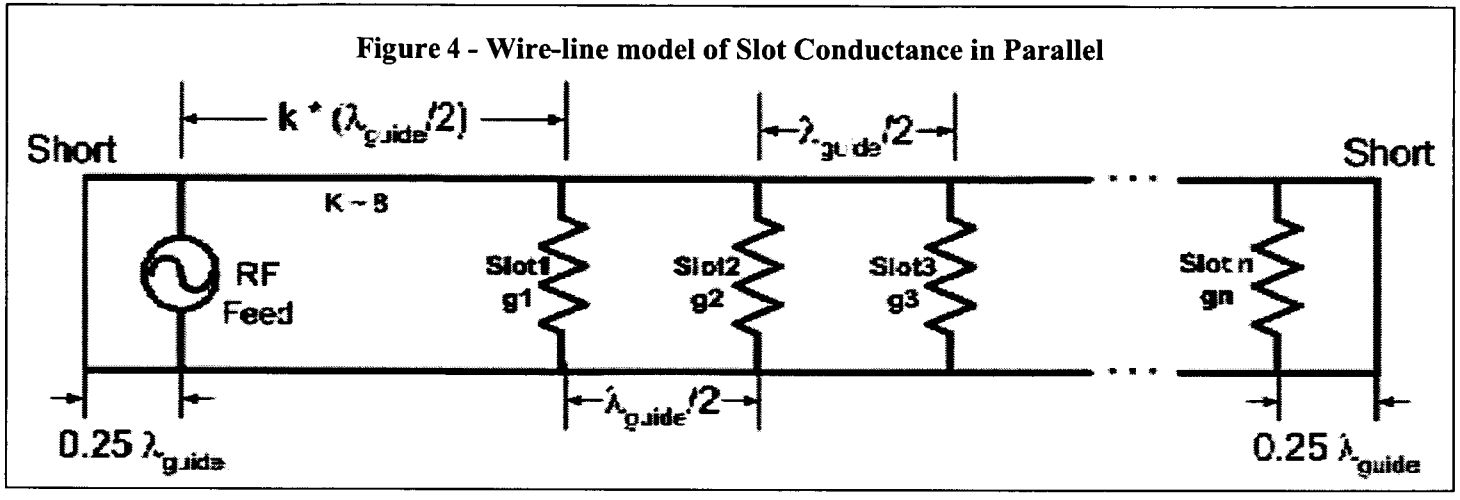

Figure 5 - Normalized Resonant Slot Conductance vs. Angle

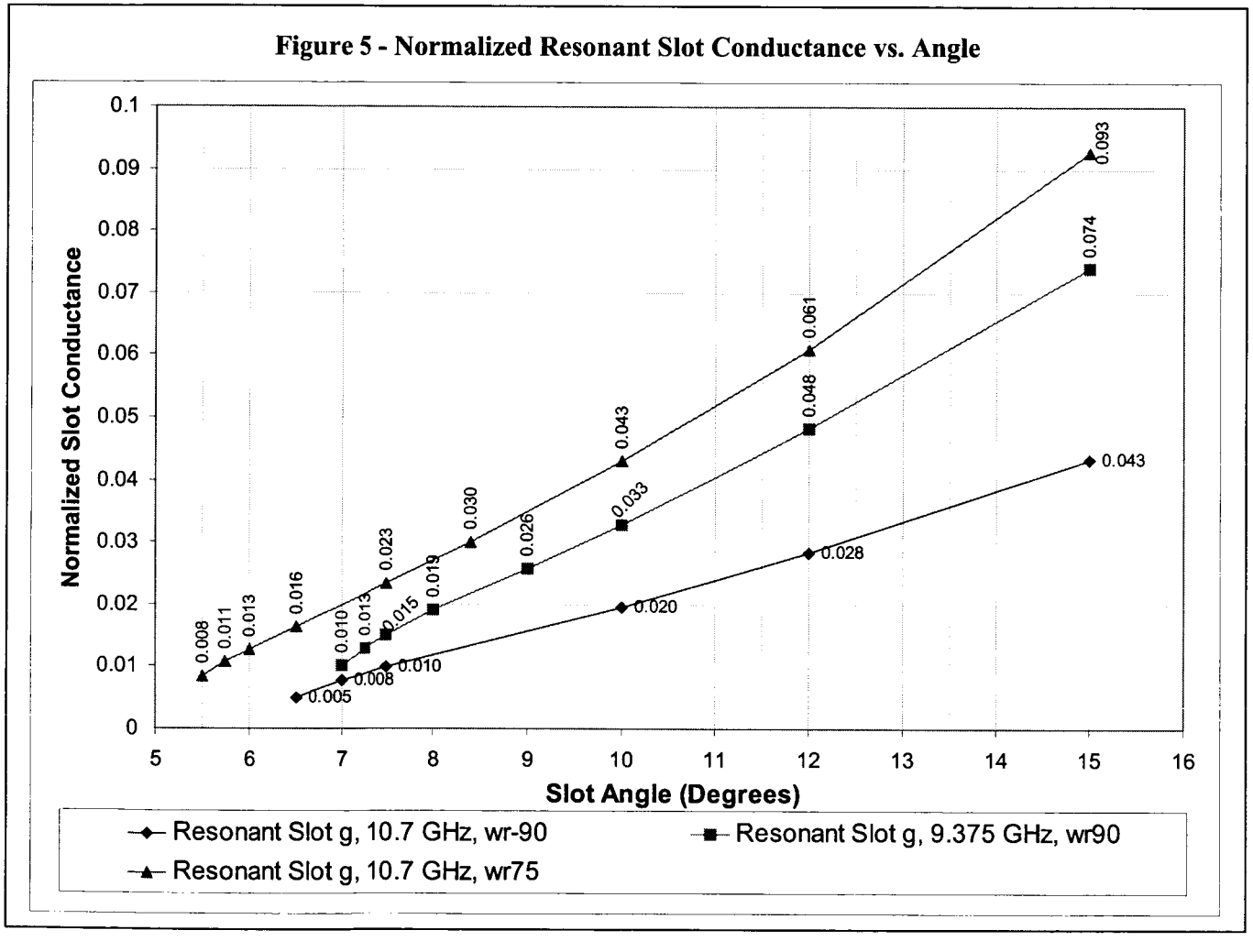

Figure 6 - Resonant Slot Depth vs. Angle

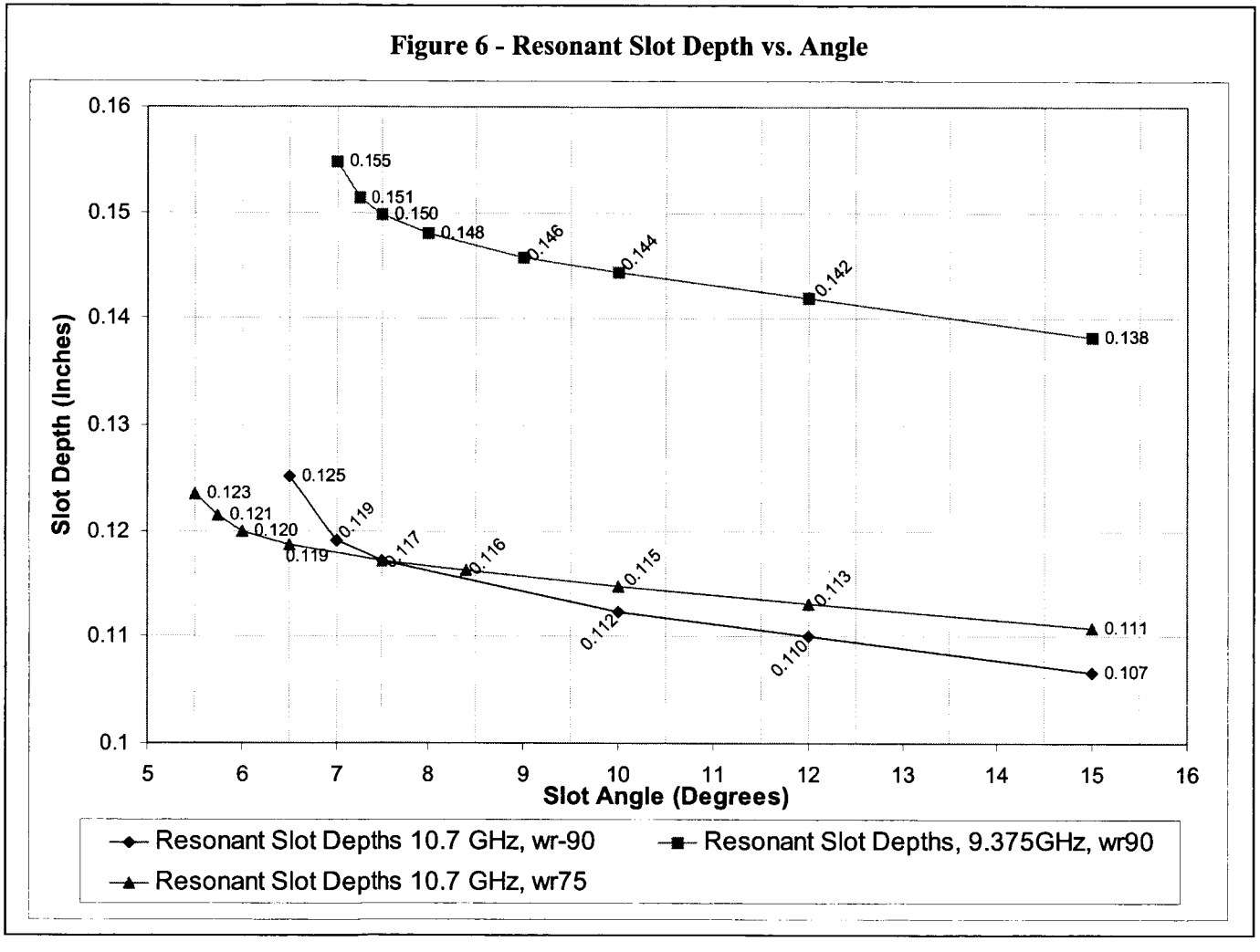

Figure 7 - Typical HFSS Model for LRR Development

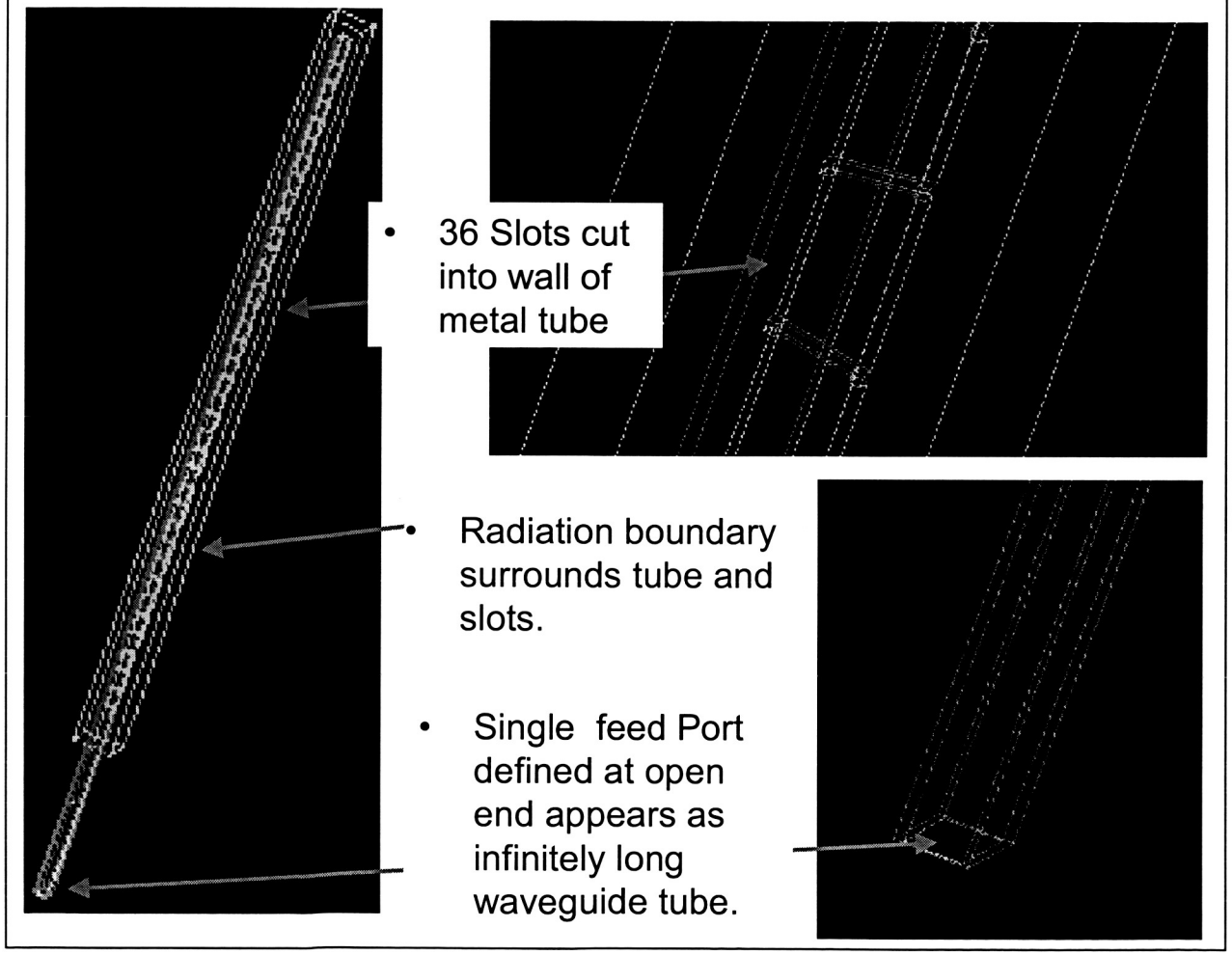

Figure 8 - HFSS Model Definitions

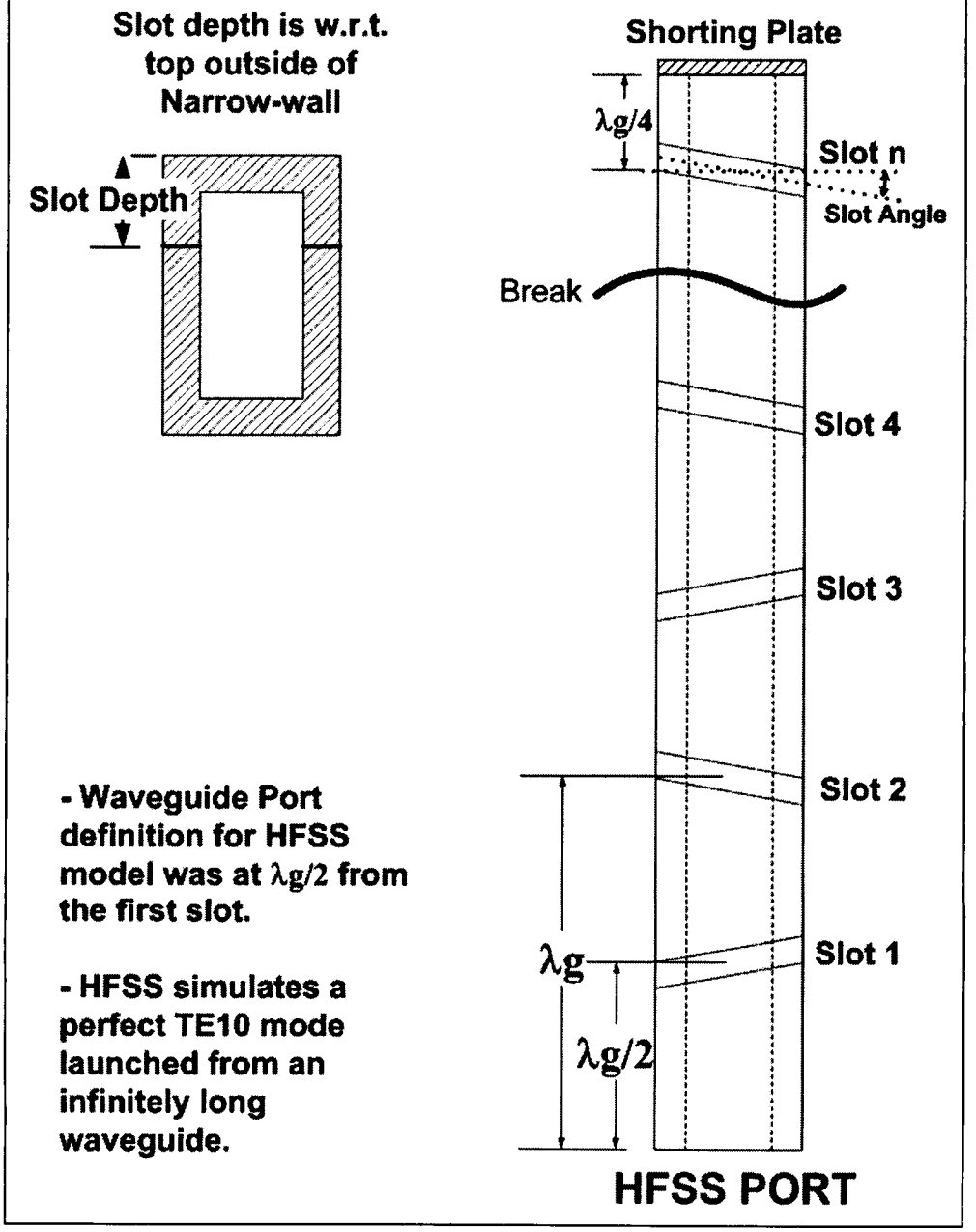

Figure 9 - Hardware Definitions

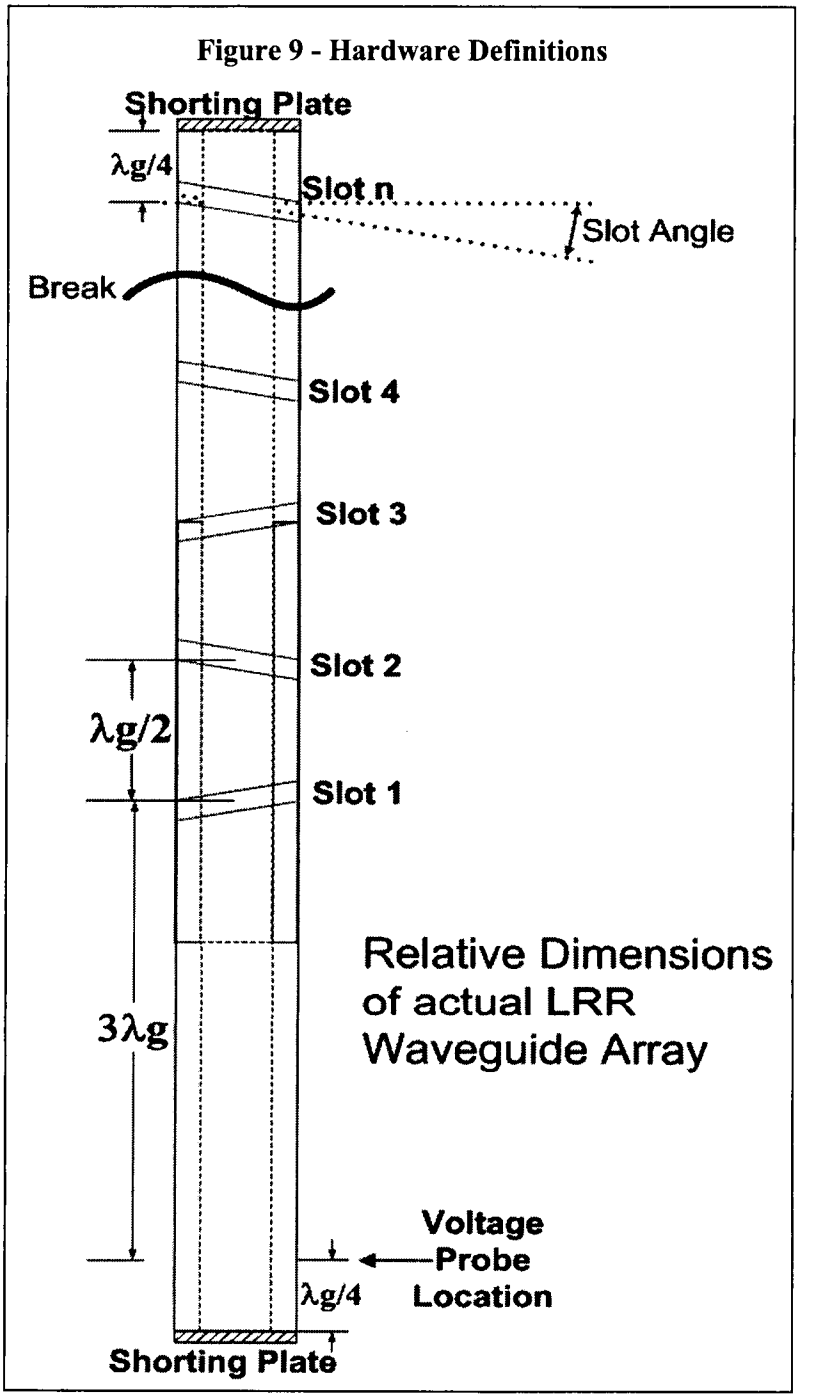

Figure 10 - Comparison of Watson's Slot Data with HFSS results

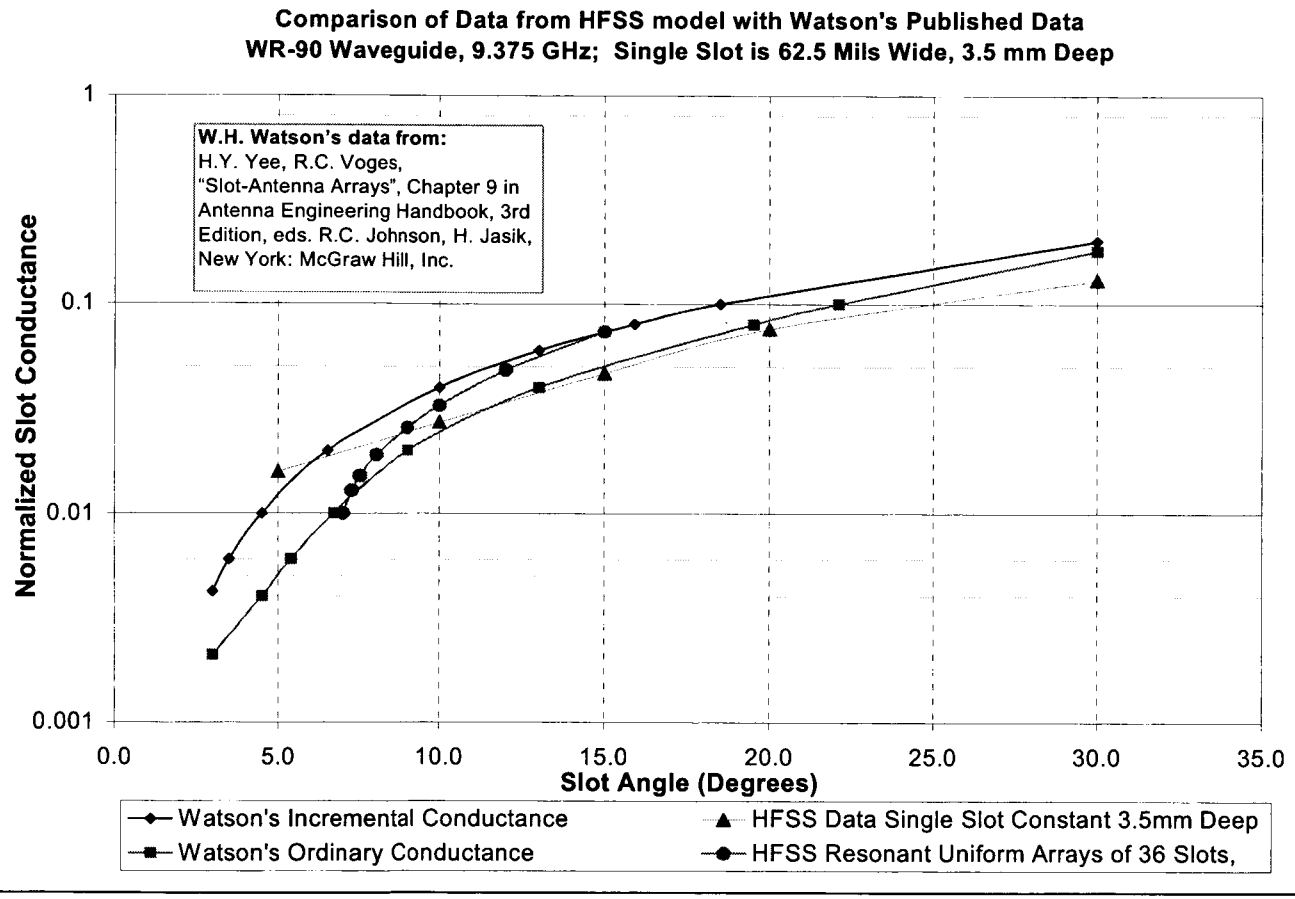

Figure 11 - VSWR for LRR X-band waveguide array

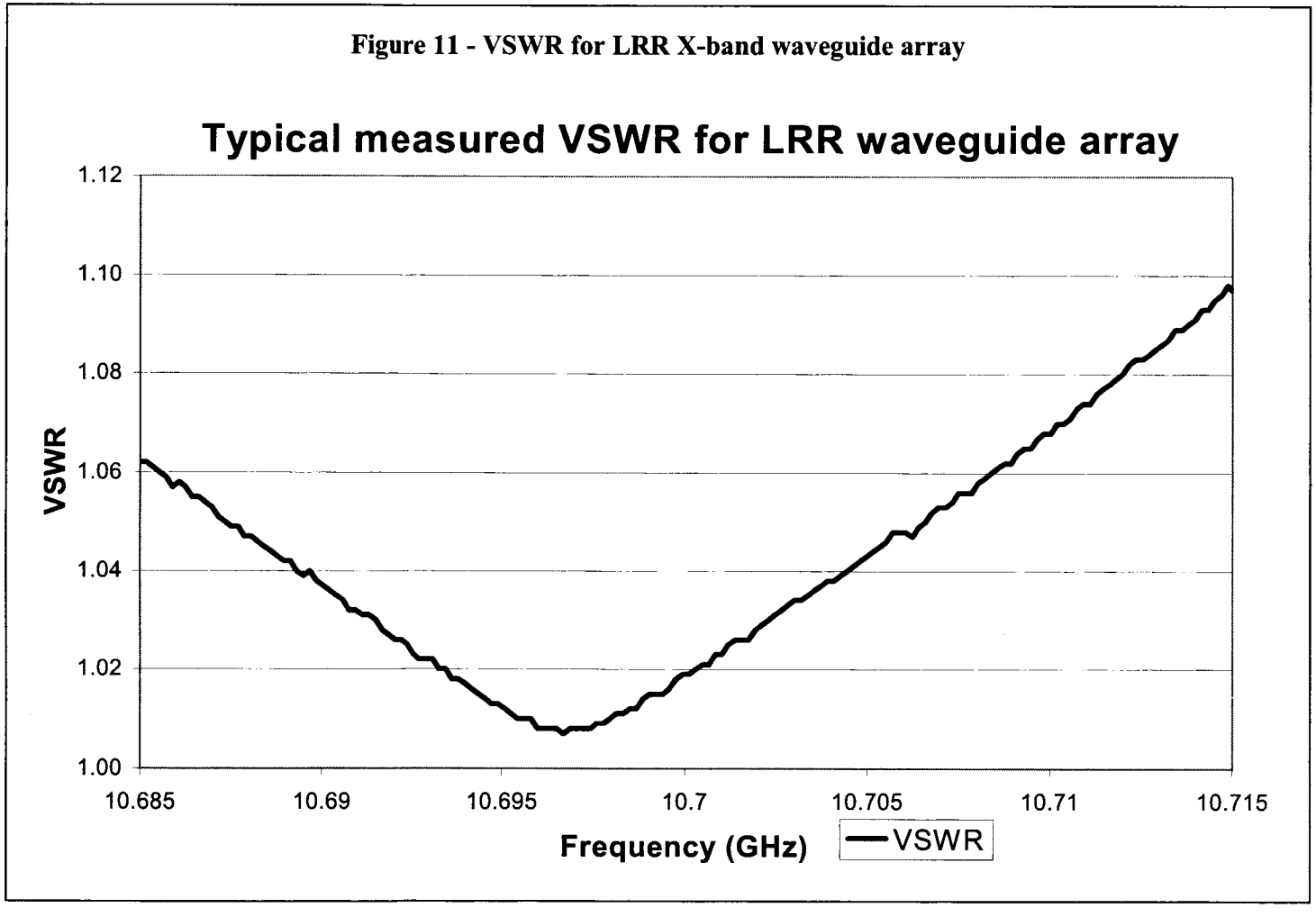

Figure 12 - Co-Polarized Pattern Comparison between HFSS and Measured

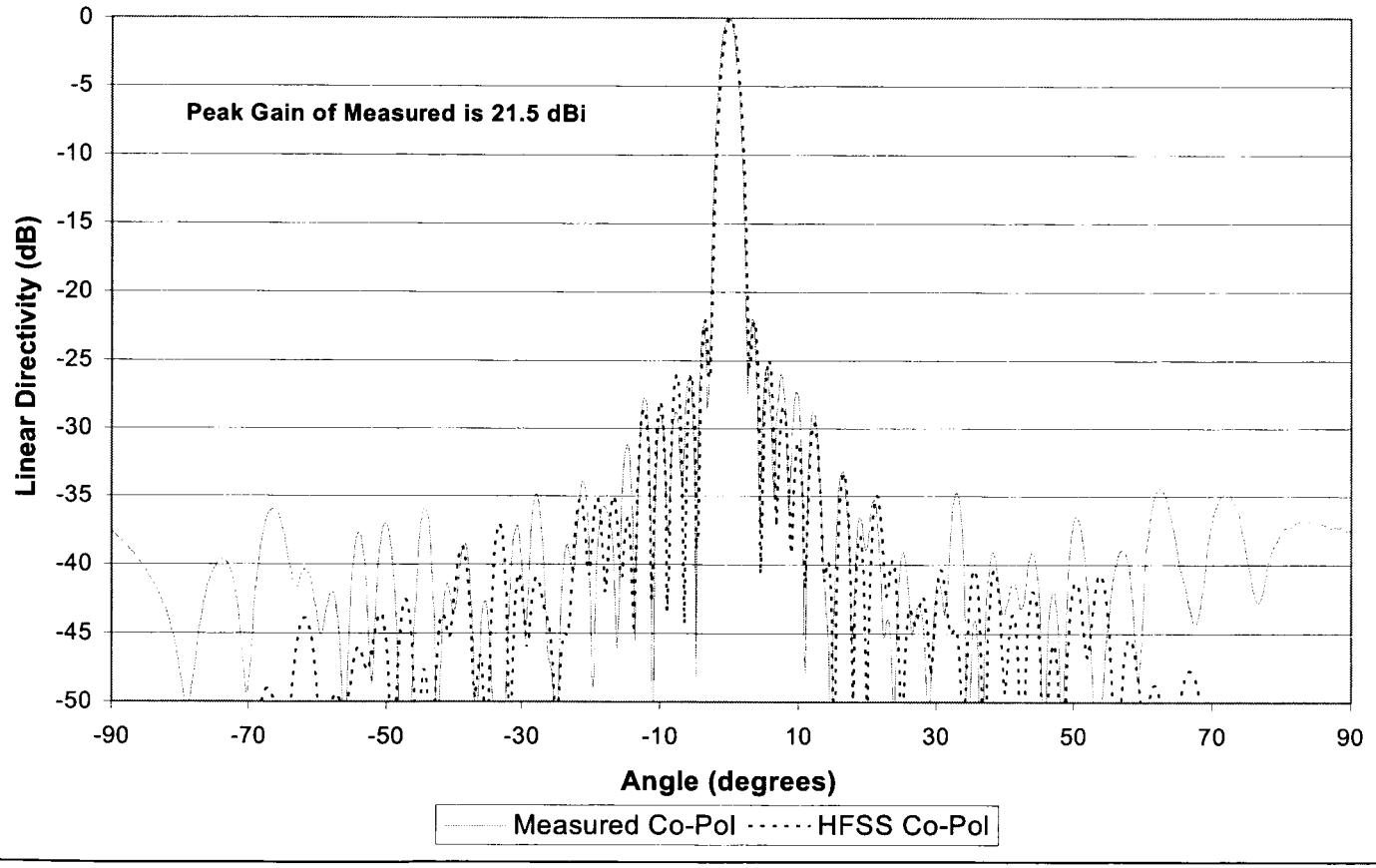

Figure 13 - Cross-Polarized Pattern Comparison between HFSS and Measured

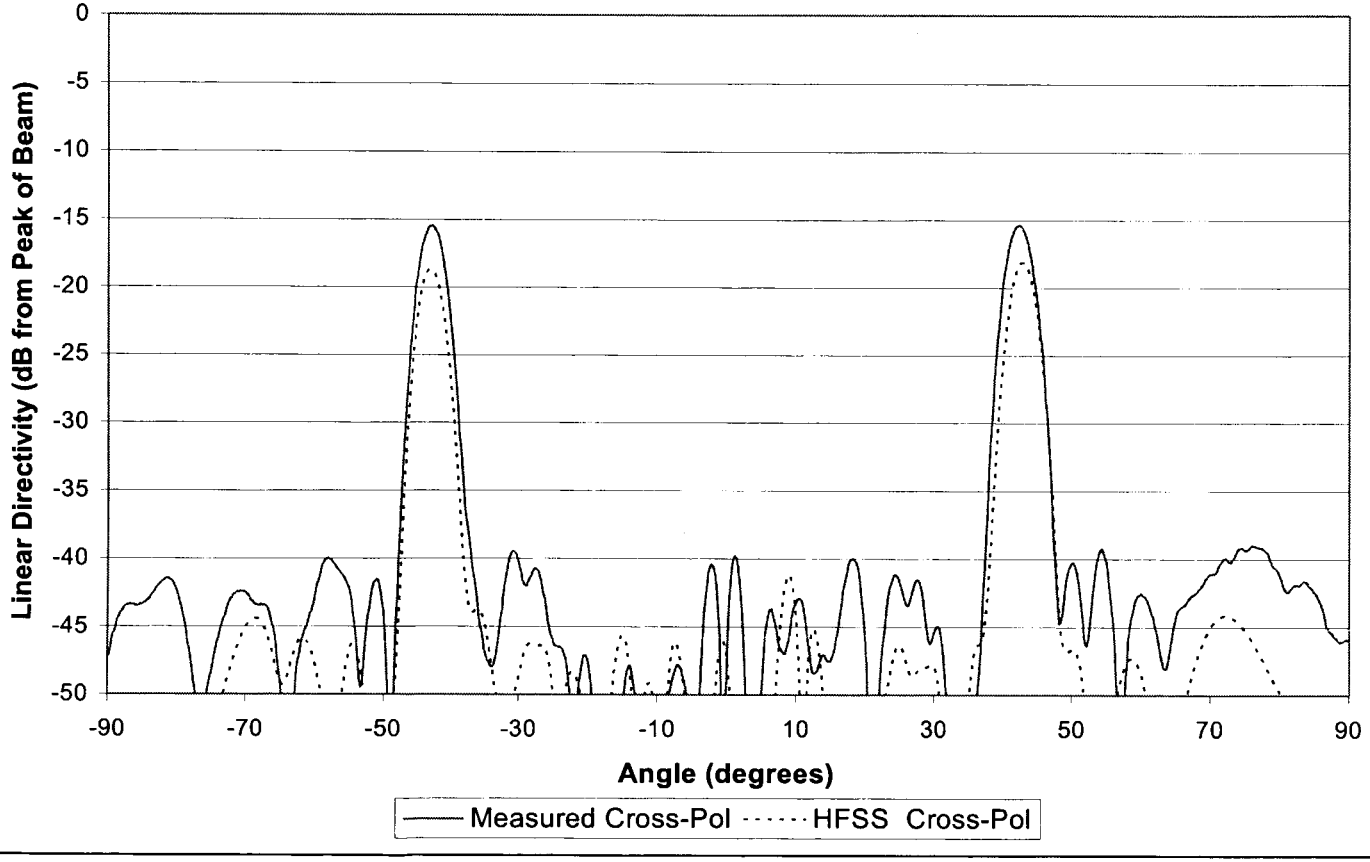

Figure 14 - Plot of Slot Conductance for Taper applied over 4 Sub-arrays using equal power division.

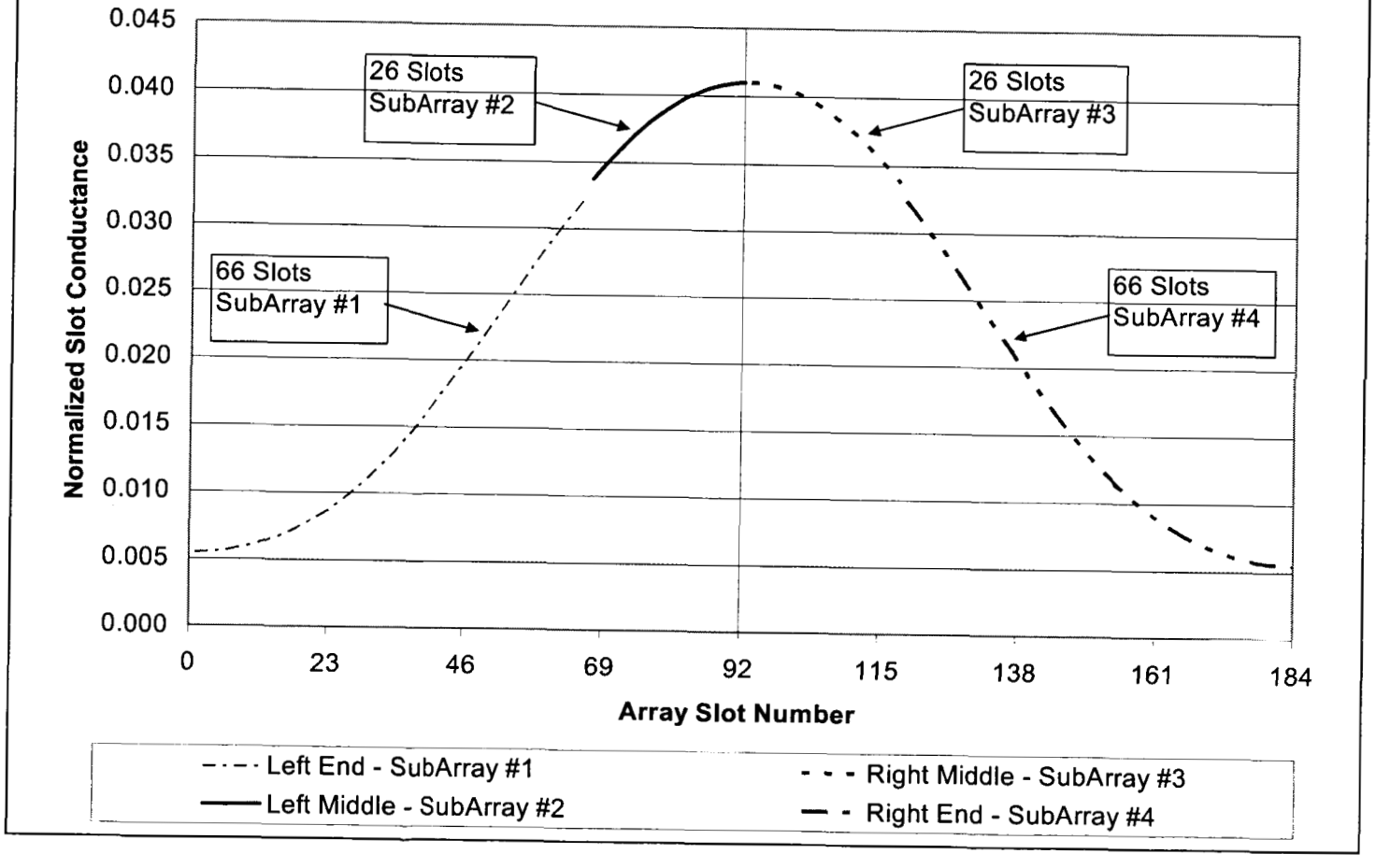

Table 1 Applying Villeneuve [11] Distribution for LRR 36-slot Array

Voltages from Analysis Data for 25 dB Taylor nbar=4	V**2 for 25 dB Taylor nbar=4	Normalized Slot Conductance g	Slot Angle Theta (degrees)	Slot Depth d (Inches)
0.370362	0.137168	0.007093694	#N/A	#N/A
0.380648	0.1448929	0.007493189	#N/A	#N/A
0.400971	0.1607777	0.00831468	5.5006	0.12347
0.430809	0.1855964	0.009598185	5.6286	0.12243
0.469316	0.2202575	0.011390698	5.8269	0.12098
0.515286	0.2655197	0.013731446	6.1417	0.11960
0.567139	0.3216466	0.016634074	6.5375	0.11864
0.62297	0.3880916	0.0200703	7.0325	0.11790
0.680637	0.4632667	0.023958008	7.5862	0.11711
0.737919	0.5445245	0.028160281	8.1497	0.11650
0.79268	0.6283416	0.032494915	8.7022	0.11596
0.843048	0.7107299	0.036755658	9.2239	0.11549
0.887542	0.7877308	0.040737786	9.7115	0.11505
0.925143	0.8558896	0.044262642	10.1310	0.11468
0.955281	0.9125618	0.047193467	10.4593	0.11441
0.97776	0.9560146	0.049440645	10.7111	0.11420
0.992621	0.9852964	0.050954966	10.8808	0.11406
1	1	0.051715366	10.9660	0.11399
1	1	0.051715366	10.9660	0.11399
0.992621	0.9852964	0.050954966	10.8808	0.11406
0.97776	0.9560146	0.049440645	10.7111	0.11420
0.955281	0.9125618	0.047193467	10.4593	0.11441
0.925143	0.8558896	0.044262642	10.1310	0.11468
0.887542	0.7877308	0.040737786	9.7115	0.11505
0.843048	0.7107299	0.036755658	9.2239	0.11549
0.79268	0.6283416	0.032494915	8.7022	0.11596
0.737919	0.5445245	0.028160281	8.1497	0.11650
0.680637	0.4632667	0.023958008	7.5862	0.11711
0.62297	0.3880916	0.0200703	7.0325	0.11790
0.567139	0.3216466	0.016634074	6.5375	0.11864
0.515286	0.2655197	0.013731446	6.1417	0.11960
0.469316	0.2202575	0.011390698	5.8269	0.12098
0.430809	0.1855964	0.009598185	5.6286	0.12243
0.400971	0.1607777	0.00831468	5.5006	0.12347
0.380648	0.1448929	0.007493189	#N/A	#N/A
0.370362	0.137168	0.007093694	#N/A	#N/A
Sums:	19.336613	1		